DEVELOPMENT OF A SYNTHETIC APERTURE RADAR

DESIGN APPROACH FOR WIDE-SWATH IMPLEMENTATION

By

B. R. Jean

September 1981

Supported by:
National Aeronautics and Space Administration
Johnson Space Center
Houston, Texas

Grant NAS 9-16102

TEXAS A&M UNIVERSITY
REMOTE SENSING CENTER
COLLEGE STATION, TEXAS

DEVELOPMENT OF A SYNTHETIC APERTURE RADAR DESIGN APPROACH FOR WIDE-SWATH IMPLEMENTATION

by

B. R. Jean

September 1981

Supported by:

National Aeronautics and Space Administration
Johnson Space Center
Houston, Texas

Grant NAS9-16102

TABLE OF CONTENTS

LIST OF FIGURES

Page

Development of a Synthetic Aperture Radar Design Approach for Wide-Swath Implementation

Final Report RSC 4272

I. INTRODUCTION

The Remote Sensing Center at Texas A&M University (TAMU) has completed the first phase of a study program for the National Aeronautics and Space Administration, Johnson Space Center (NASA/JSC) to develop an advanced synthetic aperture radar (SAR) design concept. Attributes of particular importance for the system design include wide swath coverage, reduced power requirements, and versatility in the selection of frequency, polarization and incident angle. The motivation for implementing the study program was the work previously performed at TAMU on the development of a multiple beam architecture for a synthetic aperture imaging radar.

The multiple beam configuration provides imaging at a nearly constant angle of incidence and offers the potential of realizing a wide range of the attributes desired for an orbital imaging radar for earth resources applications.

In addition to the development of a design approach for an advanced imaging radar system based upon the multiple beam concept, TAMU also provided technical evaluation support to JSC on the Advanced Synthetic Aperture Radar (ASAR) program. TAMU participated in a number of ASAR design review and planning meetings and concurred with the decision by NASA to redirect the ASAR effort away from its original ambitious objectives. Rather than prematurely attempt to implement a

multi-mode, multi-frequency, multi-polarization, and multi-application sensor, TAMU supports a more basic research and development effort that concentrates on advanced space-qualified antenna designs and in the development of system architectures that allow for efficient and timely processing of the resulting images.

The following sections of this report document the multiple beam concept and present a design example that illustrates the potential advantages of the multiple beam configuration.

II. BACKGROUND

In recent years the role of synthetic aperture radar (SAR) systems has been extended beyond gathering military intelligence to providing all weather, day or night, maps of the earth [1]. There is a growing demand among scientists in a wide range of disciplines to obtain timely, high resolution, wide swath active microwave imagery of the earth from a spacecraft platform in much the same way that optical spectra data are provided by the LANDSAT series of satellites [2]. The design of SAR systems for earth observation applications represents a different set of performance objectives from those identified for military systems, particularly when quantitative analysis of the image data is required.

Conventional SAR systems, which employ a single side-looking antenna beam, fail to satisfy many important criteria imposed when monitoring earth resources. The criteria include both image interpretation and system implementation requirements. A wide swath image formed with a single side-looking beam can be difficult to interpret because of the variation in incident angle across the scene. The radar scattering coefficient, σ°, is highly dependent upon incident angle. A large incident angle variation across the image can obscure the effects of other scene parameters on σ° [3]. There is also geometric distortion introduced across the swath because spatial resolution in this dimension is also angle dependent.

A side-looking SAR requires a high peak power transmitter for adequate signal-to-noise ratio and a long antenna in the along-track dimension for azimuth ambiguity reduction. These requirements compensate for the low pulse repetition frequency (PRF) needed for range

ambiguity avoidance. In addition, the complexity of the radar return signal makes the design of signal processors difficult and expensive.

An interesting system, called SCANSAR, has been suggested for achieving wide swath coverage that circumvents the ambiguity problems of broad fan beam antennas and also conserves transmitter power when the antenna length is constrained. The approach is that of step scanning a narrow antenna beam over the desired swath and synthesizing a synthetic aperture image within the beam at each step in the scan [4]. With careful control of the dwell time and scanning rate, continuous coverage over a wide swath can be obtained. The scanning synthetic aperture radar, however, is limited in its resolution capability and in the amount of non-coherent averaging that can be done to reduce coherent speckle in the radar image. Also the currently proposed SCANSAR does not provide a constant incident angle image.

The problems and limitations imposed by conventional side-looking SAR and the SCANSAR have led to an alternative system design concept first proposed by Claassen and Eckerman [5]. The concept is that of forming multiple real antenna beams by appropriately processing the signals from the individual elements of a single receiving array. The beams are projected along the surface of a cone as shown in Figure 1, so as to intersect the earth at a nearly constant angle of incidence. The returns from the independent beams are further processed to provide a high resolution synthetic aperture image.

This report presents the basic architecture of a Multiple Beam SAR and suggests possible implementation techniques for the various sub-systems. Antenna beam requirements are related to the image resolution and swath coverage requirements. A novel beam forming

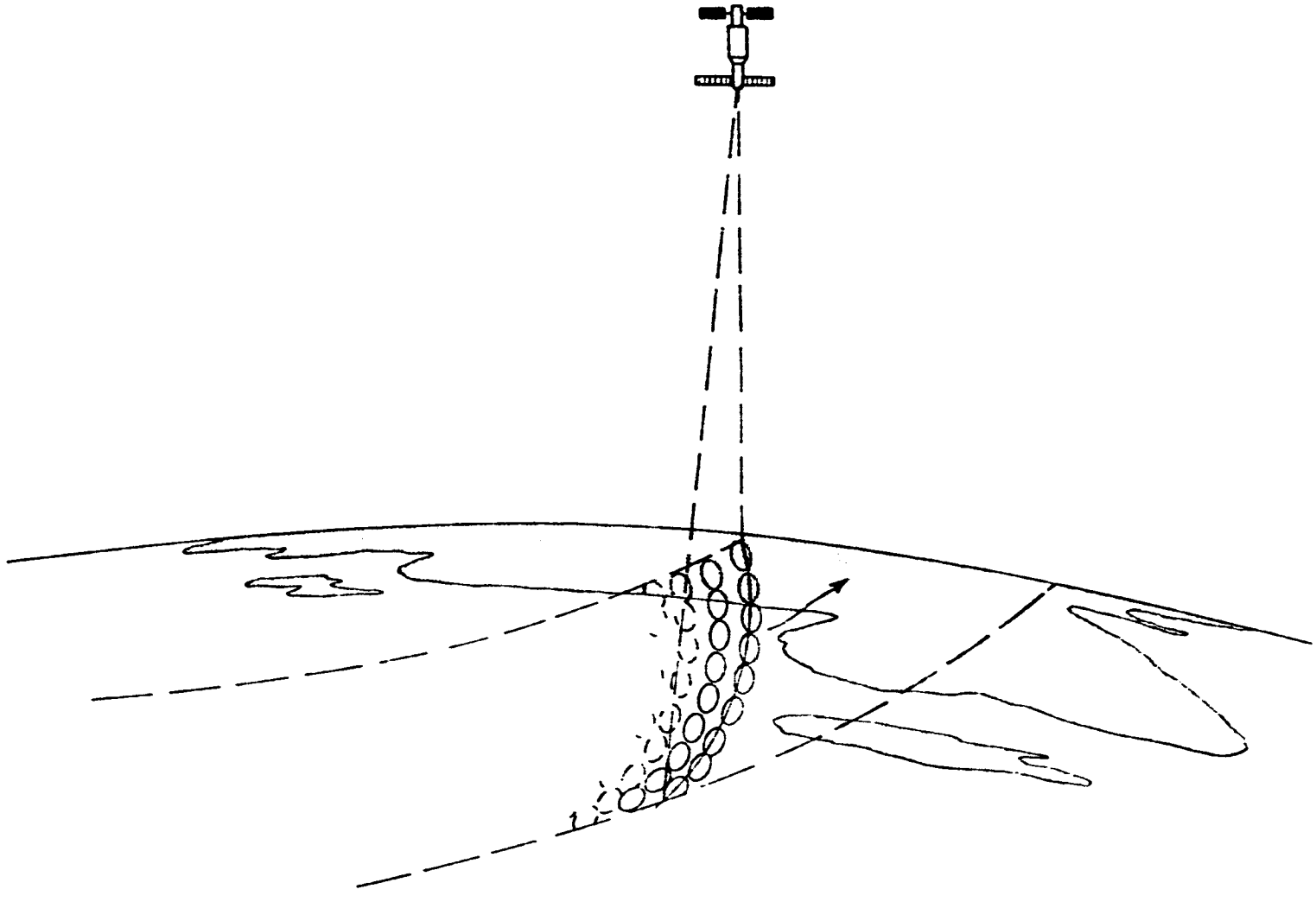

Figure 1. A multiple beam configuration for a wide swath, constant incident angle synthetic aperture radar.

technique which provides simultaneous beam formation and range compression is identified. A processing technique for SAR image formation which lends itself to real-time analog electronic implementation is also presented and analyzed.

The advantages of the Multiple Beam SAR concept, in addition to providing wide swath coverage at a nearly constant incident angle, are that it reduces the peak, and often the average, transmitter power requirements, it gives considerable relief from the range and azimuth ambiguity suppression constraints, and it employs an antenna which may be more easily deployed in space. The penalty associated with the multiple antenna beam configuration is the additional signal processing required to form the beams. For the modest resolutions often associated with orbital mapping of earth resources, the increased signal processing burden required for beam formation can be somewhat offset by the reduced complexity in the SAR image formation processor.

III. THE MULTIPLE BEAM CONFIGURATION

The antenna for the Multiple Beam SAR is mounted vertically. It consists of a rectangular array which is oriented with respect to the vehicle velocity vector as depicted in Figure 2. The array is rotated about its vertical axis (the z-axis in Figure 2) to point the direction of ϕ_0. Multiple beams are formed about ϕ_0 to give angular coverage from ϕ_{min} to ϕ_{max}. The vertical dimension of the array is designed to produce a narrow elevation beamwidth. This contrasts with the side-looking configuration which requires a broad elevation beam.

In the horizontal dimension, signals from the individual elements are combined by a beam formation processor to yield output signals corresponding to multiple, independent antenna beams, each having the gain of the full array. These signals are further processed to form a synthetic aperture image within each of the real antenna beams. A functional block diagram of the Multiple Beam SAR is shown in Figure 3.

The incident angle, swath width, and resolution requirements for the SAR system constrain the design of the antenna array. Consider first the inside portion of the swath (ϕ near ϕ_{min}). The available synthetic aperture length is set by the elevation beamwidth, β_e. The relationship may be written approximately as

$$vT_a = \frac{R_0 \beta_e}{\cos\phi \cos\theta_0}$$

where vT_a = aperture integration length

(velocity times aperture integration time)

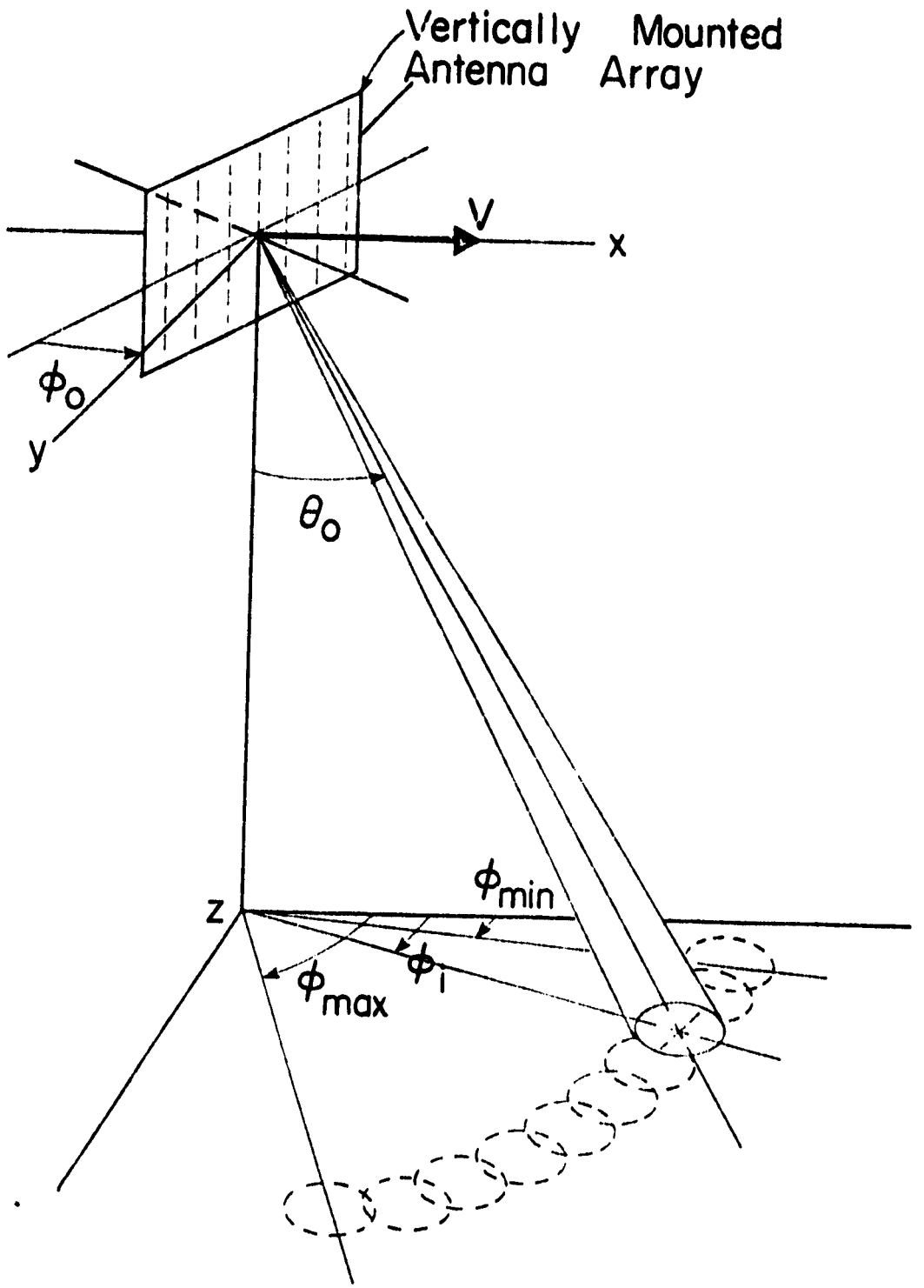

Figure 2. Antenna orientation and imaging geometry for the Multiple Beam SAR.

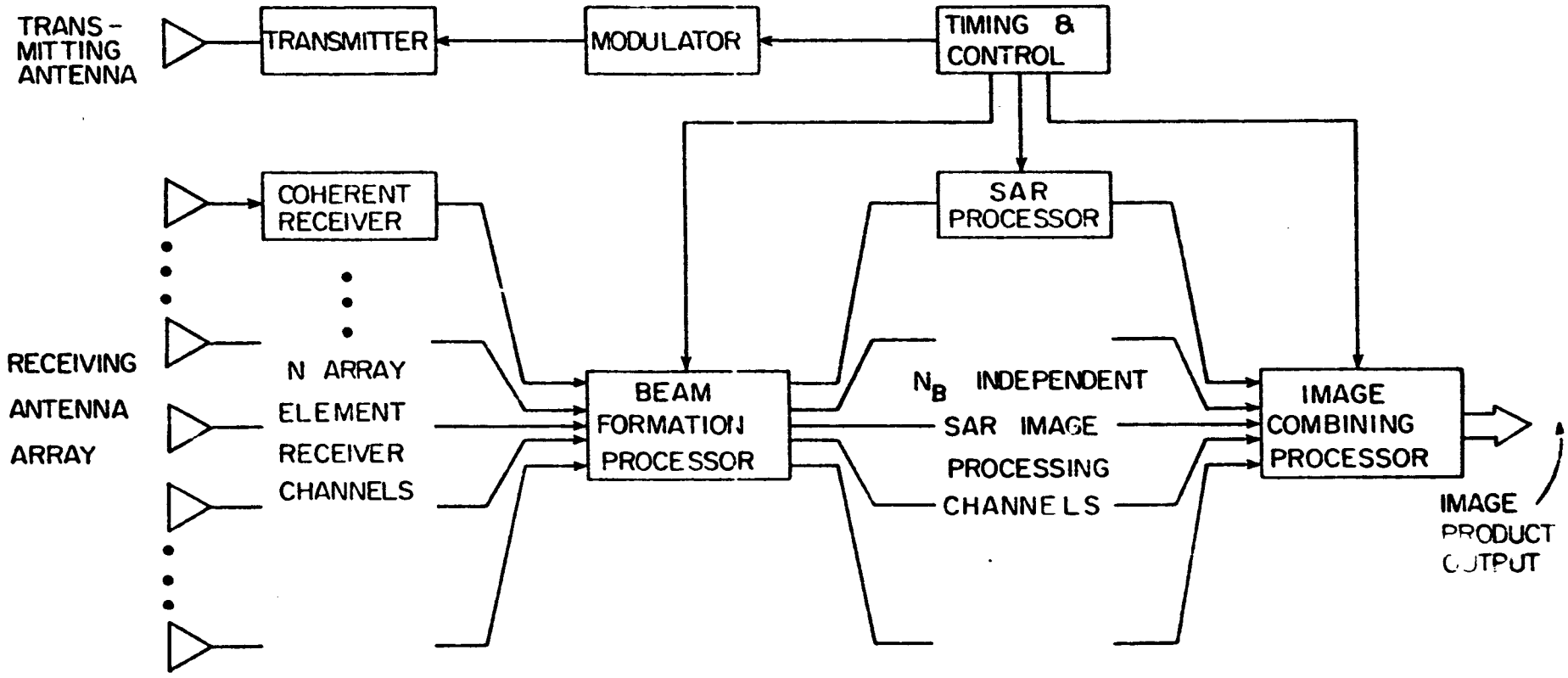

Figure 3. Block diagram of a Multiple Beam SAR system.

R_0 = range to the beam center

ϕ = azimuth angle variable

θ_0 = incident angle (elevation angle variable)

If N_ℓ independent looks are required, with an along-track resolution ρ_x, the aperture integration length must be such that

$$vT_a > \frac{N_\ell \lambda R_0}{2 \rho_x (1-\sin^2\theta_0 \cos^2\phi)}$$

where λ is the wavelength [6]. Note that ρ_x is the "along track" resolution, not the azimuth resolution. The use of ρ_x here makes sense, since a target passes through the beam in the along track or x direction. A minimum value for β_e is

$$\beta_e \geq \frac{N_\ell \lambda \cos\theta_0 \cos\phi_{min}}{2 \rho_x (1 - \sin^2\theta_0 \cos^2\phi_{min})}. \qquad (1)$$

The maximum elevation beamwidth is determined by range ambiguity constraints. Expressed in terms of ΔR, the unambiguous slant range interval, the bound on β_e is

$$\beta_e < \frac{\Delta R \cot\theta_0}{R_0}$$

Slant range interval and the along-track resolution must be traded via limits placed on the PRF in sampling the Doppler spectrum. The Nyquist sampling rate for range offset processing may be expressed in terms of the vehicle velocity, along-track resolution and number of looks.

$$PRF \geq \frac{vN_\ell}{\rho_x}$$

To avoid range ambiguities, the slant range interval and the PRF are related as

$$\Delta R < \frac{c}{2PRF} - c\tau$$

where c is the electromagnetic wave velocity of propagation, and τ is the transmitted pulse width. The Doppler spectrum and range ambiguity limits may be combined in a single expression as

$$\Delta R < \frac{c\rho_x}{2vN_\ell} - c\tau.$$

Thus, the maximum elevation beamwidth may be written in terms of the along-track resolution, the number of multiple looks, the incident angle, the vehicle velocity, and the transmitted pulse width. The resulting expression is

$$\beta_e < \frac{c \cot\theta_0}{R_0} \left\{ \frac{\rho_x}{2vN_\ell} - \tau \right\} \qquad (3)$$

The limits imposed by (1) and (3) are rather broad and allow considerable flexibility in specifying β_e. The upper limit on β_e is a significant constraint for a side-looking system since wide swath coverage requires a large elevation beamwidth. This limit is seldom of concern for the Multiple Beam configuration, since wide swath coverage is obtained in the azimuth dimension, not in range. In general, the elevation beamwidth will be chosen to be as small as possible to take advantage of the corresponding large antenna gain.

The considerations for determining the horizontal dimension specifications are similar to those for the vertical dimension. An additional requirement is that the beamwidth in ϕ must be wide enough

at each beam position to assure overlapping coverage across the entire swath. For large ϕ, it is the horizontal beamwidth which determines the synthetic aperture length. This forces a lower limit on β_h which is similar to the requirement on β_e as expressed in (1). That is, β_h is bounded by the appoximate inequality.

$$\beta_h > \frac{N_\ell \lambda/\sin \phi_{max}}{\rho_x(1 - \sin^2\theta_0 \cos^2\phi_{max})}.$$

Again it is desirable to achieve as small a beamwidth as possible to reduce power requirements.

The familiar expression for the signal-to-noise ratio of a synthetic aperture radar may be applied to the Multiple Beam SAR with slight modification [7]. The signal-to-noise ratio may be written as

$$\frac{S}{N} = \frac{P_{avg} D_{ht} D_{hr} D_e^2 \sigma^0 \rho_r}{N_B 8\pi k\ T_0 F_h R^3 \lambda\ v \sin\theta} \qquad (4)$$

where P_{avg} = the average transmitted power

σ^0 = cross-section per unit area

ρ_r = slant range resolution

k = Boltzman's constant

T_0 = reference temperature

F_n = receiver noise figure

D_{ht} = horizontal dimension of the transmitting antenna

D_{hr} = horizontal dimension of the receiving antenna

D_e = receiving and transmitting antenna elevation dimension

N_B = number of beams

The transmitting antenna beamwidth in the horizontal dimension is roughly N_B times the beamwidth of the receiving antenna, where N_B is the number of beams. The signal-to-noise ratio thus appears to be reduced by the factor $1/N_B$ from that of a competing single beam system. However, for comparable swath coverage from a single beam system, both transmitting and receiving beamwidths would be larger by a factor of N_B for an overall $1/N_B^2$ signal-to-noise ratio reduction. Thus in terms of antenna gain alone, the multiple beam system appears to offer roughly a factor of N_B signal-to-noise ratio improvement over a single beam system giving comparable swath coverage. However, this signal-to-noise ratio advantage is lost in the beam formation network since the overall processing bandwidth must be N_B times that of a single beam system.

A signal-to-noise ratio advantage that is not lost however, is that due to the allowable increase in the PRF. The PRF can be increased by the same amount that the elevation beam-width is reduced. Typically the repetition rate can be increased by a factor of at least N_B over a conventional single beam side-looking system. Because of the accompanying increase in the PRF, increasing the length of the antenna in the elevation dimension has a twofold impact on reducing the peak power requirement. For wide swath designs this savings in peak power can be significant.

In addition to reducing the peak power requirement, the multiple beam configuration can significantly reduce the dynamic range requirement of the receiver. Because the image is formed at a nearly constant incident angle, the large variation in σ^0 as a function of angle no longer becomes a factor in specifying the dynamic range of

the system. As a practical matter, this also leads to an improvement in signal-to-noise ratio for systems employing an analog to digital (A/D) converter. A reduction in dynamic range for a fixed number of bits in the A/D leads to a reduction in quantization noise. If quantization noise is not a limiting factor then the number of bits can be reduced.

IV. A DESIGN EXAMPLE

To illustrate the potential advantages of the multiple beam configuration over conventional side-looking designs, a rough set of calculations have been made for a system which would be somewhat comparable to the Seasat SAR [8]. The relevant specifications for the Seasat SAR are listed in Table 1 below.

Table 1

SEASAT-A SAR SYSTEM CHARACTERISTICS (after Jordan [8])

Satellite Altitude	800 km
Wavelength	0.235 m
RF Bandwidth	19 MHz
Pulse Repetition Frequency	1463 to 1640 Hz
Time Bandwidth Product	634
Radar Transmitter Peak Power	1000 watts
Radar Transmitter Average Power	55 watts
Radar Antenna Dimensions	11 by 2.3 m

The design procedure for specifying the multiple beam SAR starts with determining the elevation beamwidth. From (1) the minimum value of elevation beamwidth is calculated to be 1.12°. It is not advisable to design for this minimum beamwidth although it would be desirable to do so. If the antenna length in the elevation dimension can be as large as the Seasat antenna length in a horizontal dimension, that is 11 meters, then an elevation beamwidth of 3.16° can be achieved. The antenna beam must be steered downward by approximately 70° from the broadside direction to provide a nominal 20° incident angle.

The minimum spacecraft altitude is dictated by the swath width specification and the angular extent over which beams are formed. If beams are formed within the angular region from ϕ = 10° to ϕ = 50°, then the minimum altitude is computed to be about 464 km. For this

design, a value of 500 km will be taken as nominal. With the specification of the beamwidth and altitude, the unambiguous slant range interval can be computed and is found to be approximately 10.7 km. From (2), an upper limit on the PRF can be calculated. The maximum PRF is found to be about 14 KHz.

The horizontal dimension design requires computation of the element spacing for the horizontal array. A maximum element spacing of about 1 meter or roughly 4.3 λ is required to scan an angular region of 40°.

A number of tradeoffs must be considered before an optimum selection for the number of beams and the number of elements in the horizontal array can be made. For the sake of brevity, we assume that four elements will do an adequate job. The element width must provide an elemental pattern which will control the grating lobes. An element width of approximately .9 meters should be adequate. The overall antenna size turns out to be about 4 x 11 meters. This is somewhat larger in the narrow dimension than the Seasat antenna but is not an unreasonable size.

If beams are formed symetrically about the antenna broadside then the beam pointing angles, measured in ϕ, occur at ϕ = 18, 26, 34, and 42 degrees. The width of each beam will be on the order of 20°. This beamwidth figure takes into account aperture weighting to reduce side lobes levels to acceptable values. A 20° beamwidth provides adequate overlap to insure contiguous coverage across the entire swath.

The antenna beamwidths define the Doppler ambiguity constraints. A maximum Doppler bandwidth of about 5 KHz can be expected. The PRF

can therefore be selected from the range of about 5 to 14 KHz. A nominal value of 10 KHz seems reasonable for the calculations which follow.

The required average power can be computed from (4) using parameter values comparable to those for the SEASAT radar. The minimum signal-to-noise ratio is chosen to be 10 dB, the receiver noise figure is estimated at 6 dB and the minimum average value of σ^o at 20° is -13 dB. A nominal value for velocity is 7.5 km/sec. The slant range resolution corresponding to 1.9 MHz is 15.79 m.

From these values the total average transmitter power is found to be 4.24 watts while the peak power is 12.69 watts. Even if these values are adjusted to take into account the higher altitude of the SEASAT radar, they would increase only by a factor of 4.1. The peak power savings achieved over the SEASAT design is on the order of 13 dB.

While many other factors would enter into play in a detailed system design study, the power reduction indicated here is significant and demonstrates one principal advantage of the multiple beam configuration.

V. BEAM FORMATION TECHNIQUES

There are a number of ways to implement multiple beam formation. Both digital and analog techniques for forming multiple beams following coherent reception of the return signal by the individual horizontal element receiver channels are available [9, 10, 11, 12].

Analog beam forming requires time or frequency multiplexing of the individual element receiver outputs. Johnson [9] has shown that if the antenna element signals are time multiplexed, then the antenna beam signals are frequency multiplexed. Conversely, frequency multiplexed elements produce output signals that are multiplexed in time. A novel implementation utilizing the chirp Z-transform (CZT) algorithm is shown in Figure 4. The CZT implementation incorporates time multiplexing of the element signals precisely as described by Johnson. However, by virtue of the Fourier transform operation, the resulting frequency multiplexed beam signals are transformed into time multiplexed beam signals. An additional outcome of utilizing the CZT algorithm is that range compression is accomplished within the same processing operation.

The CZT technique requires that the input signal be premultiplied by a chirp signal of the form $e^{-j1/2\mu t^2}$. The multiplied signal is then passed through a dispersive filter whose impulse response is a similar chirp waveform of the opposite sense [13]. A second multiplication by $e^{-j1/2\mu t^2}$ following the chirp filter removes a residual quadratic phase factor, if required.

In the beam formation processor of Figure 8, the premultiplication function occurs in the transmitter. The transmitter waveform is a linear FM pulse of duration T seconds with a chirp rate of $-\mu$ radians per second squared.

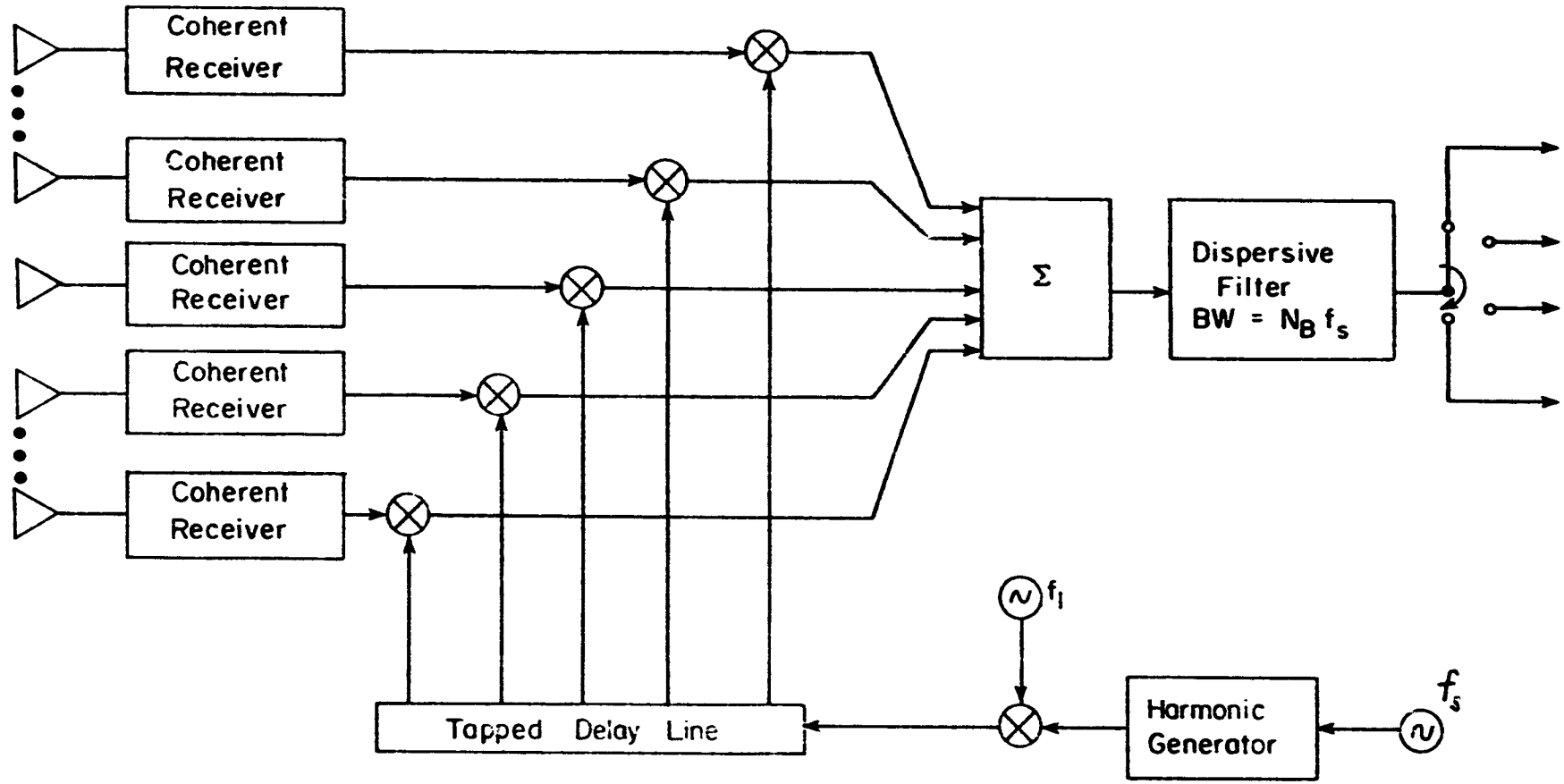

Figure 4. An analog beam formation processor based upon the CZT algorithm.

The receiving array element outputs are multiplexed at a sampling rate of ω_s. The sampling frequency must be greater than the Nyquist rate in order to provide adequate time separation between the beams. The time separation between beams must be large enough to allow the entire range interval to be processed for one beam direction before the next beam signal appears.

The bandwidth of the multiplexed signal is determined by ω_s and the number of beams formed. It is roughly equal to $N_B\omega_s/2\pi$ HZ. Since the processing filter must be matched to the trnasmitter linear FM rate, the impulse response duration T_f of the filter can be computed as

$$T_f = \frac{N_B \omega_s}{2\pi B} T$$

where B is the RF bandwidth in HZ.

Jean has shown that the output signal from the processing filter is of the form [6].

$$E_{out} = T\, e^{-1/2 j\mu t^2} \sum_m \frac{\sin \frac{\mu T}{2}\left(t - \frac{m\omega_s}{\mu}\right)}{\frac{\mu T}{2}\left(t - \frac{m\omega_s}{\mu}\right)}$$

$$\cdot \sum_n E_n\, e^{jn\left[kd_n \sin\upsilon_0 \sin\phi - \frac{2\pi m}{N_B}\right]}$$

where E_n = amplitude of the signal from the nth element.

k = wave number $(2\pi/\lambda)$

d_h = horizontal element spacing.

The sin x/x term in the first summation appears due to the pulse

compression operation. It is noted that the output for each beam occurs at time

$$t = \frac{\pi w_s}{\mu} .$$

The second summation indicates the formation of the individual antenna beams.

A potential disadvantage of the CZT beam forming processor is that it imposes another limit on the PRF of the transmitter. If the full unambiguous range interval is to be processed, the PRF must be reduced so that all N_β range intervals can be processed before the return from the next succeeding pulse arrives at the receiver. This need not be a serious limitation for the Multiple Beam SAR, however, provided that the antenna elevation beamwidth can be made sufficiently narrow. The problem may also be circumvented by employing a range gating operation prior to beam formation to allow only the range interval of interest to enter the CZT processing filter.

VI. IMAGE FORMATION PROCESSING FOR THE MULTIPLE BEAM SAR.

Aside from the beam formation operation, the processing steps required to form the synthetic aperture image are essentially the same for both the mulitple beam and conventional sidelooking radars. A processing scheme is presented below which is particularly well suited to the multiple beam configuration. The processor architecture takes advantage of the fact that the imaging geometry naturally conforms to the range-Doppler coordinates of the radar.

Swath coverage is obtained in the Doppler dimension, along contours of constant range. Sidelooking systems achieve wide swath coverage in the range dimension along a contour of constant Doppler, usually along the zero Doppler line. For sidelooking systems the Doppler compression operation constitutes the major processing burden. Because the Doppler chirp rate is a function of range, many Doppler filters are req red to process a wide swath image. A separate Doppler compression operation must be done for each range resolution interval.

The approach taken in processing the multiple beam image results in having to process only a few range bins. More significant than the reduction in the number of range bins is the fact that Doppler compression operation can now be accomplished with a single Doppler filter. This comes about because the imaging geometry provides a nearly constant Doppler chirp rate across the entire swath. The filter bandwidth is determined by the Doppler bandwidth within a single antenna beam. The Doppler dimension resolution is determined by the number of Doppler samples that are integrated by the filter.

An architecture for a Doppler dimension processor is shown in Figure 5. The configuration is based upon a processing technique suggested by Claassen [5]. The processor has a master computer which provides control of the range gating operation and calculates the adjustments required for motion compensation. The function of the range gate controller is to assure that the signal samples are collected in a precisely controlled sequence. The Doppler signal history from which a single set of azimuth resolution elements are formed is collected from a narrow strip of terrain through the center of the beam. A complete sample set corresponds to the return signal collected from a strip roughly equivalent to a single range bin. The range gate for a given strip is continuously advanced so as to capture successive pulses from the same patch of terrain as the vehicle advances toward the patch.

To obtain continuous imaging along the swath several range intervals must be tracked simultaneously. The number of range bins required is roughly given by

$$N_{rb} = \frac{N_\ell v T_a}{\rho_x}.$$

Figure 6 provides an illustration of the range tracking operation. Consider the strip of terrain through the center of the beam that corresponds to the range bin centered on range R_1. At time $t_1 = 2R_1/c$, after the first pulse is emitted, the sample corresponding to this constant range contour is acquired. The second

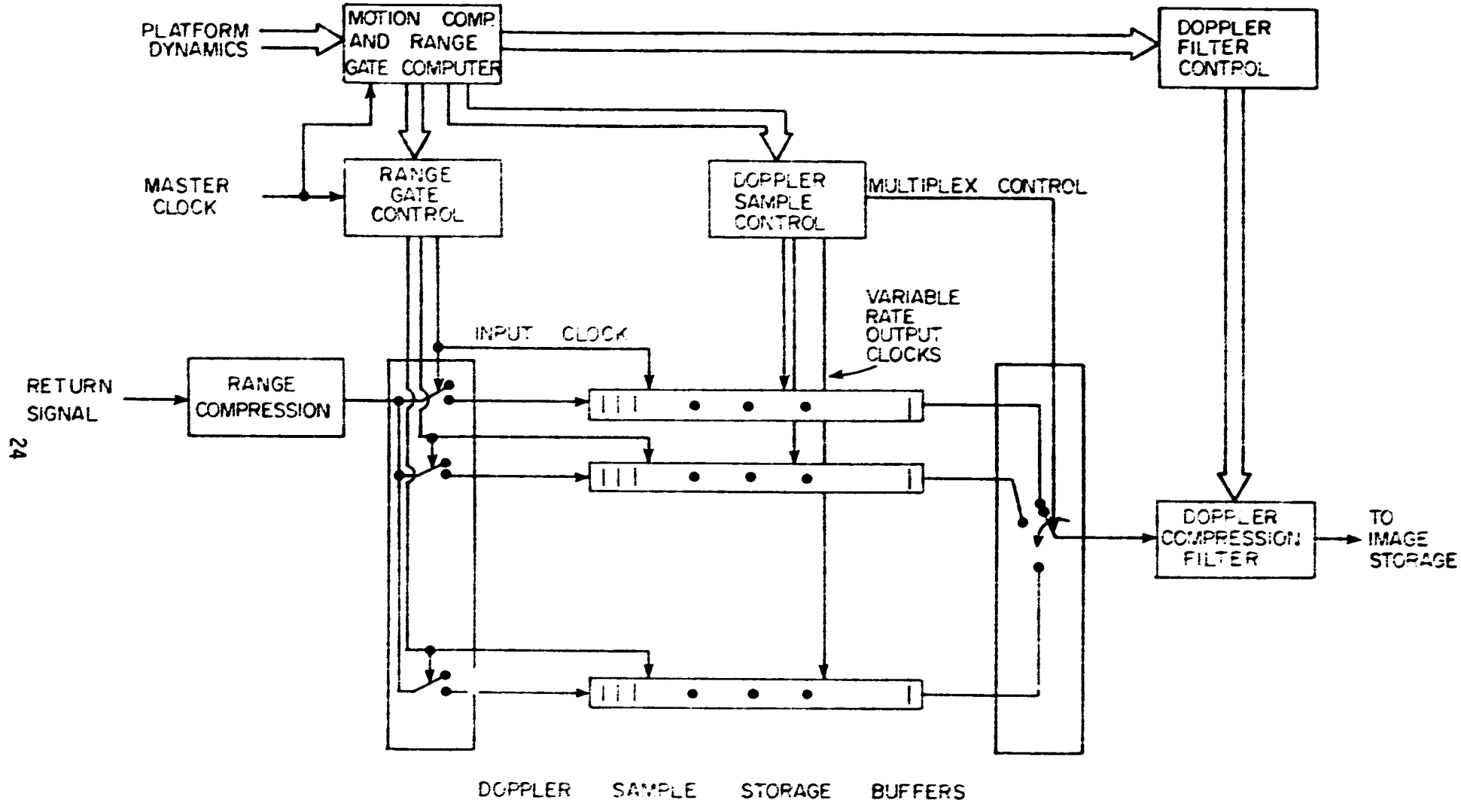

Figure 5. Architecture of a Doppler processor for the Multiple Beam SAR.

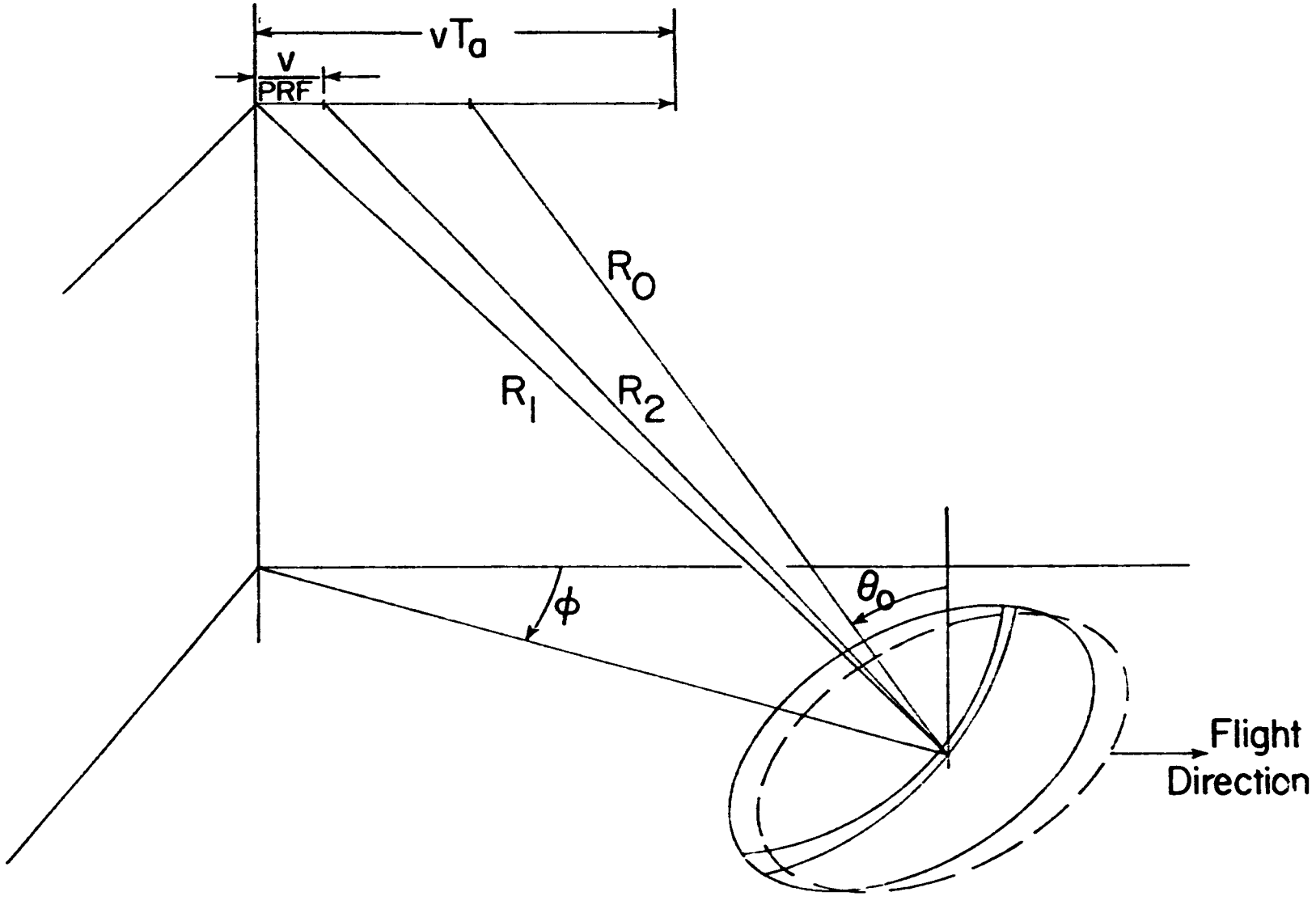

Figure 6. Range tracking geometry required for obtaining the Doppler signal history from a given azimuth strip within a single beam. (Beam size and aperture length are greatly exagerated.)

pulse emitted by the transmitter occurs at t = 1/PRF. The range to the center of the strip being sampled has decreased from R_1 to R_2, where R_2 is approximately

$$R_2 = R_1 - \frac{V}{PRF} \sin\theta_o \cos\phi_i .$$

The range gate for the second sample in the Doppler signal history of this strip of terrain must occur earlier in time by an amount Δt_i given by

$$\Delta t_i = \frac{2V \sin \theta_o \cos\phi_i}{cPRF} .$$

This range gate adjustment is repeated for each successive pulse until the required number of samples have been collected.

It must be noted that while the sample time can be adjusted to account for the decrease in range to the center of the strip, the range bins rotate about this center point as the radar advances along the flight path. There is also an increase in the curvature of the range bins as the range to the strip decreases. This rotation and change in curvature introduces a range tracking error at the ends of the strip which depends upon the velocity, the integration time, the range to the target, and the antenna beamwidth. The ground range error can be computed by approximating the strip as a straight line segment of length

$$\ell = R\beta_h$$

where R is the nominal range to the center of the strip and β_h is the azimuth beamwidth. The line segment rotates by an amount

$$\Delta\phi = \frac{vT_a \sin\phi_i}{R\sin\theta_0}$$

The ground range error is approximately

$$\Delta R_g = 1/2 \ \ell\Delta\phi .$$

If this error is to be less than ρ_g, the ground range resolution, then the following inequality must hold,

$$vT_a < \frac{2\rho_g \sin\theta_0}{\beta_h \sin\theta_i}.$$

The Doppler Compression Operation

To form the individual image resolution elements, in the azimuth dimension the collected samples must be processed by the Doppler compression filter. As noted before, the bandwidth of this filter is governed by the Doppler signal bandwidth across the antenna beam, whereas the frequency resolution is governed by the integration time, i.e. by the number of samples that are collected.

The identity of each resolution element appearing at the filter output is expressed in terms of the time delay of the signal through the filter. If ω_{dj} is the offset frequency of the jth Doppler resolution element, referenced to the beam center, and μ_d is the linear FM rate, then this time delay may be written as

$$\tau_j = \frac{\omega_{dj}}{\mu_d}.$$

It is not necessary to perform the Doppler compression function at the same rate that data are collected. Since all of the data are available in storage, the data may be processed at a rate much faster than the real-time acquisition rate [14].

The adjustments necessary for motion compensation are also easily incorporated into the Doppler filtering operation. Variation in vehicle velocity create corresponding variations in the Doppler chirp rate. The chirp rate of the stored data can be dynamically corrected to compensate for non-uniform velocity by simply varying the rate at

which the data are extracted from the sample storage buffer [13]. Since the Doppler chirp rate is very nearly constant over the entire imaged swath, this form of motion compensation is applied to all the data at once.

This chirp rate adjustment technique implies the use of an analog filter. Other filter implementations are possible with appropriate resampling of the data after the signal has been converted to an analog form. Of course an all digital processor is possible, but such would lack the simplicity of the variable clock rate motion compensation scheme.

Continuous Coverage and Multiple Look Processing.

As noted previously, several range bins must be tracked concurrently to assure continuous coverage along the swath. The processor must begin tracking a new range interval each time the vehicle advances by a distance equal to one ground range resolution element. This interval must be tracked until the vehicle has advanced by one aperture integration length. If a multiple look image is desired this interval must be tracked for a number of aperture lengths equal to the number of multiple looks N_ℓ.

The multiple look images from a given strip within the beam will not overlay precisely due to the previously identified range error which occurs at the ends of the strip. If the same criterion for the maximum allowable range error is applied for multiple look registration as was specified for the range error in sampling the Doppler signal history, then the number of looks which can be combined without range error correction is limited by

$$N_\ell < \frac{2\,\rho_g\,\sin\theta_o}{\beta_h \sin\theta\; v\; T_a} \quad .$$

VII. CONCLUSIONS AND RECOMMENDATIONS

The multiple beam synthetic aperture design concept has been presented and compared with conventional side-looking architectures. Calculations have shown that the multiple beam design offers considerable savings in transmitter power requirements at the expense of additional processing requirements. Other attributes of the design include the ability to image at a nearly constant incident angle while achieving wide-swath coverage. The multiple beam configuration also employs an antenna system that can preserve the polarization properties of the return signal, provided the antenna elements themselves can provide good polarization isolation.

A processing scheme has been presented for the multiple beam SAR which offers the potential of on-board, real-time image formation. The processor is relatively simple in concept and, it is reasonable to expect that it can be implemented with current CCD and SAW technologies.

It is recommended that future development efforts be concentrated in two specific areas. First, emphasis should be placed upon antenna design technology to develop antenna structures that can provide good polarization isolation (> 25 dB, integrated over the full beam), and that can be incorporated into the multiple beam configuration.

Secondly, additional work in SAR processor technology is required, not only for the multiple beam system, but for imaging radars in general. The processing techniques presented in this request should be pursued by way of computer simulation, followed by actual implementation in the laboratory using existing devices that are commercially available.

REFERENCES

[1] R. E. Mathews, ed., "Active Microwvae Users Workshop Report," NASA Conference Publication 2030, Johnson Space Center, Houston, Texas, August 1976.

[2] R. E. Mathews, ed., "Active Microwave Workshop Report," NASA SP-376, Scientific and Technical Information Office, National Aeronautics and Space Administration, Washington, D. C., 1975.

[3] B. J. Blanchard, "Analysis of Synthetic Aperture Radar Imaging," Final Report, 3359-2, Remote Sensing Center, Texas A&M University, June 1977.

[4] Moore, R. K., J. P. Claassen and Y. H. Lin, A. Scanning Spaceborne Synthetic-Aperture Radar (SCANSAR) and a Combined Microwave Radiometer Sensor, University of Kansas Remote Sensing Laboratory, Submitted to IEEE Transaction of AES, January 1980.

[5] Claassen, J. P. and J. Eckerman, "A System Concept for Wide Swath Constant Incident Angle Coverage," Proceedings of the Synthetic Aperture Radar Technology Conference, New Mexico State University, Las Cruces, New Mexico, March 1978.

[6] B. R. Jean, "Multiple Antenna Beam Formation Techniques for Synthetic Aperture Radar," Technical Report RSC-99, Remote Sensing Center, Texas A&M University, December 1978.

[7] L. J. Cutrona, "Synthetic Aperture Radar," Chapter 23, Radar Handbook, M. I. Skolnik, ed., McGraw Hill Book Company, New York, 1970, pp. 23-1 to 23-25.

[8] R. Jordan, "The Seasat-A Synthetic Aperture Radar Design and Implementation," Proceedings of the Synthetic Aperture Radar Technology Conference, New Mexico State University, Las Cruces, New Mexico, March, 1978.

[9] M. A. Johnson, "Phased Array Beam Steering by Multiplex Sampling," Proceedings of the IEEE, Vol. 56, No. 11, pp. 1801-1811, November 1968.

[10] S. Haykin, "Efficient Implementation of Multiple Beam Samples for Continuously Scanned Array Antennas," Electronics Letters, Vol. 12, No. 2, p. 48, January 22, 1976.

[11] D.E.N. Davies, "A Fast Electronically Scanned Radar Receiving System," Journal Brit. I.R.E., pp. 305-321, April 1961.

[12] W. P. Delaney, "An RF Multiple Beam-Forming Technique," IRE Transactions on Military Electronics, pp. 179-186, April 1962.

[13] R. C. Williamson, "Properties and Applications of Reflective-Array Devices," Proceedings of the IEEE, Vol. 64, No. 5, pp. 702-710, May 1976.

[14] J. P. Claassen, "The Potential of Incorporating a Synthetic Aperture Radar Capability Into the Meteorological Radar Facility," Technical Report RSC-87, Remote Sensing Center, Texas A&M University, May 1977.